Magnetic Excitations in Strongly Correlated Electrons
J. Phys. Soc. Jpn. **69** (2000) Suppl. B. pp. 10–15

Incommensurate spin correlations in lightly-doped $La_{2-x}Sr_xCuO_4$

Masaaki MATSUDA

The Institute of Physical and Chemical Research (RIKEN), Wako, Saitama 351-0198

(Received November 24, 1999)

A review is given of the neutron scattering studies in the lightly-doped $La_{2-x}Sr_xCuO_4$, which exhibits insulating spin-glass behavior. Most remarkable feature is that the static spin correlations are incommensurate at low temperature across the entire insulating spin-glass region. The incommensurate positions imply a one-dimensional spin modulation which is rotated by 45° from that in the superconducting phase.

KEYWORDS: $La_{2-x}Sr_xCuO_4$, spin-glass, stripe ordering, neutron scattering

§1. Introduction

The phase diagram of $La_{2-x}Sr_xCuO_4$ has been explored and it has been shown that the magnetic properties evolve dramatically with Sr doping.[1] The parent material La_2CuO_4 shows three-dimensional (3D) long-range antiferromagnetic ordering below ~325 K.[2,3] When Sr is doped in the material, the 3D antiferromagnetic ordering quickly disappears and, as originally predicted by Aharony *et al.*,[4] the Néel state is replaced by a spin-glass phase. In this phase elastic magnetic Bragg rods, originating from two-dimensional (2D) spin correlations, develop gradually as shown by Sternlieb *et al.*[5] and Keimer *et al.*[6] In particular, Keimer *et al.* found that the magnetic peaks are almost elastic and relatively sharp in Q in $La_{1.96}Sr_{0.04}CuO_4$.

In superconducting samples, an essential feature is that the magnetic correlations become incommensurate (IC)[8,7,9,10]. Detailed studies on the hole concentration dependence of the low energy magnetic excitations have been performed by Yamada *et al.*[7] They find that the incommensurability (δ) is almost linear with hole concentration (x) with $\delta \simeq x$ below x ~0.12 as shown in Fig. 1.

Recently, static magnetic ordering has been observed in superconducting $La_{1.88}Sr_{0.12}CuO_4$ (Refs.[11,12]) with the magnetic onset temperature near T_c. The elastic magnetic peaks are observed at the same IC positions as those of the magnetic inelastic peaks. A model that describes this behavior is that of stripe ordering of spin and charge (hole) density waves as observed in $La_{2-y-x}Nd_ySr_xCuO_4$ (Ref.[13]). In this case the charge and, concomitantly, spin stripes run along the a_{tetra} or b_{tetra} axis (collinear stripe). Thus, magnetic ordering takes place in the $La_{2-x}Sr_xCuO_4$ system with various levels of hole doping.

In this paper, we report on what is the nature of the static magnetic behavior in the spin-glass phase of $La_{2-x}Sr_xCuO_4$. The most interesting issue is the relationship between the spin-glass, the stripe, and the low temperature magnetic phase in the superconducting samples. A review is given of the elastic neutron scattering studies on the spin-glass phase of $La_{2-x}Sr_xCuO_4$ in the wide hole concentration range $0.02 \leq x \leq 0.05$. It is interesting to clarify how the long-range 3D antiferromagnetic ordering disappears and is replaced by the spin-glass behavior and then superconducting properties appear with hole doping.

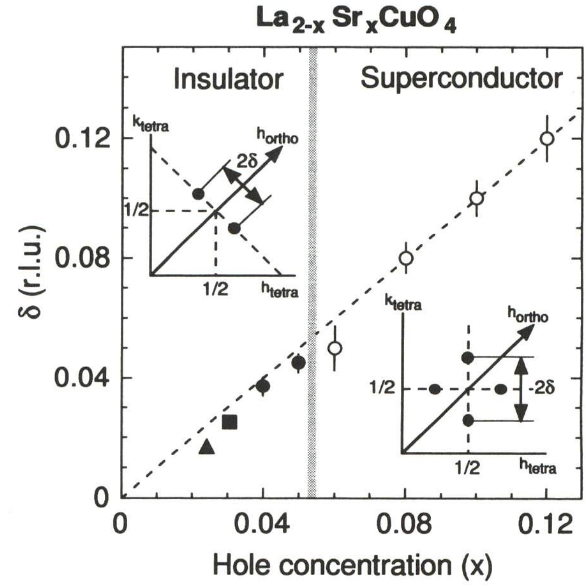

Fig. 1. Hole concentration (x) dependence of the splitting of the IC peaks (δ) in tetragonal reciprocal lattice units. Open circles indicate the data for the inelastic IC peaks reported by Yamada *et al.* [7]. Filled circles and square are the data for the elastic IC peaks reported by Wakimoto *et al.* [14,15,24]. The filled triangle is obtained by Matsuda *et al.* [17]. The broken line corresponds to $\delta = x$. The insets show the configuration of the IC peaks in the insulating phase (diagonal stripe) and the superconducting phase (collinear stripe) [17].

The format of this paper is as follows: The static properties in the spin-glass phase are presented in Sec. 2. First, the spin correlations in the CuO_2 plane are summarized. The spin structure perpendicular to the CuO_2 plane is then presented. Preliminary results of the magnetic excitation measurements are shown in Sec. 3.

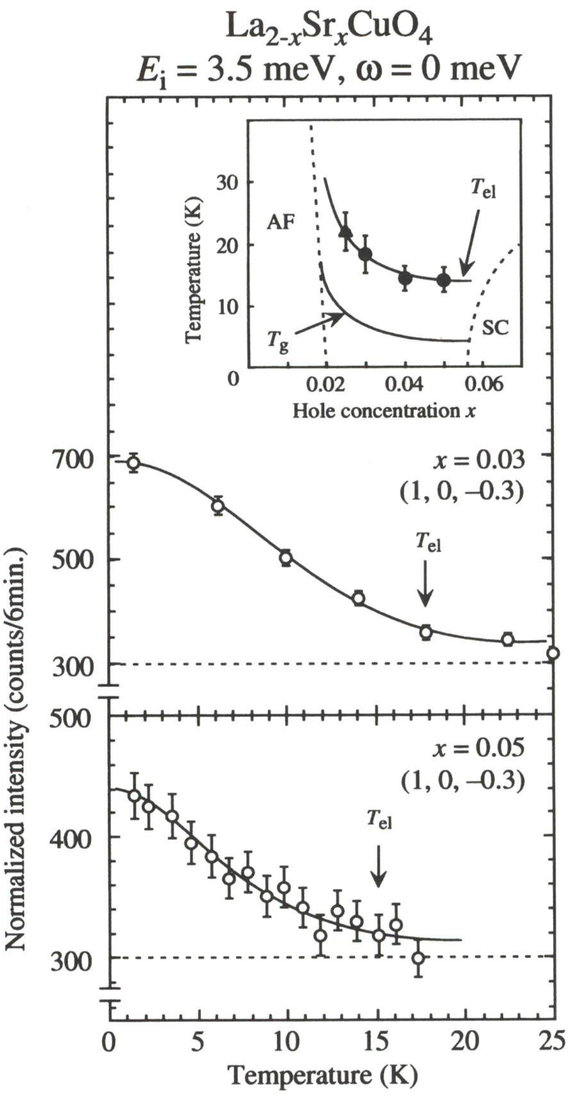

Fig. 2. Temperature dependence of the elastic peak intensity measured at $(\frac{1}{2}, \frac{1}{2}, -0.3)$ in $La_{2-x}Sr_xCuO_4$. The dashed lines indicate background levels. The solid lines are guides to the eye. The inset figure shows hole concentration dependence of the ordering temperature determined from neutron elastic measurements T_{el} and from magnetic susceptibility measurements T_g. After Wakimoto *et al.* [14].

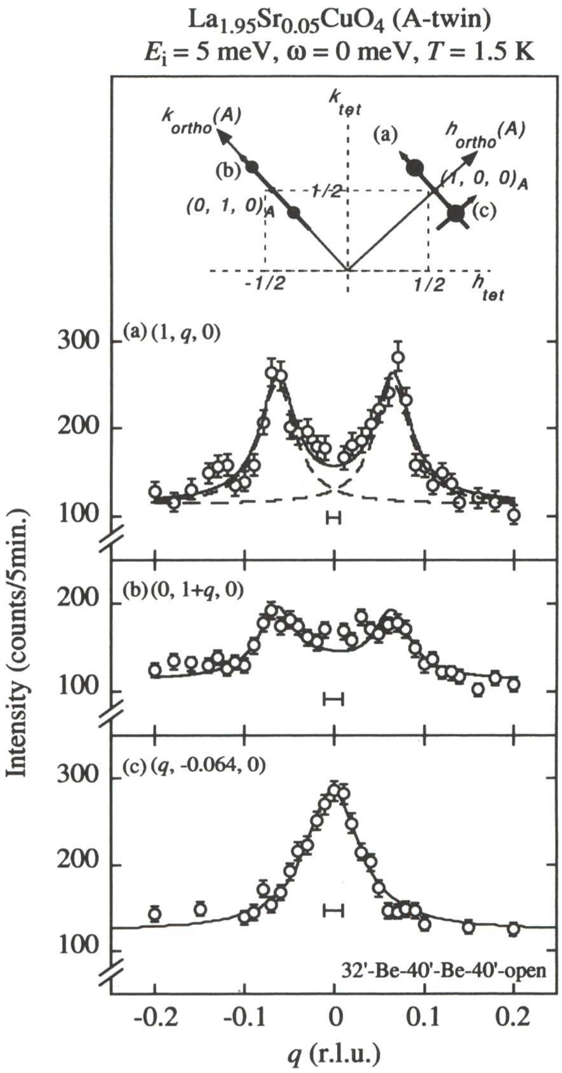

Fig. 3. Elastic scans around (1,0,0) and (0,1,0) at 1.5 K in $La_{1.95}Sr_{0.05}CuO_4$. Scan trajectories are illustrated in the inset. The solid lines are the results of the calculation. The small horizontal bars indicate the resolution full width. After Wakimoto *et al.* [15].

§2. Static properties

2.1 Incommensurate spin correlations in the CuO_2 plane

Very recently, Wakimoto *et al.* studied the magnetic properties in the spin-glass phase ($0.03 \leq x \leq 0.05$) in detail elucidating the hole concentration dependence of the transition temperature and the spin correlations.[14] As shown in Fig. 2, the elastic magnetic signal gradually develops at the (π, π) position at low temperatures. The ordering temperature determined from the neutron elastic measurements is systematically higher than that from magnetic susceptibility measurements, indicating that the magnetic signal is quasi-elastic and slightly fluctuating components (~0.01 meV) are included. Most remarkable finding in their study is new type of IC spin correlations in $La_{1.95}Sr_{0.05}CuO_4$. This was first interpreted as the rotation of 45° from the parallel satellites in the superconducting phase[8,7,13]. Then the careful examination of the intensity profiles revealed[15] that there are only 2 satellite peaks along b_{ortho} while in superconducting compounds the IC peaks are located parallel to both the a_{tetra} and b_{tetra} axes as shown in Fig. 3. The magnetic peaks are observed at the IC positions $(1,\pm\epsilon,0)$ and $(0,1\pm\epsilon,0)$ with $\epsilon \sim 0.064$. The magnetic correlations strongly suggest the diagonal stripe, in which the stripe runs along the b_{ortho} axis. These results suggest that static magnetic correlations change from diagonal to collinear stripe at x=0.055±0.005 where the insulator-to-metal transition occurs.

The next step is to clarify whether the IC magnetic correlations persist throughout the spin-glass phase down to the critical concentration of x=0.02 for 3D Néel ordering. Matsuda *et al.* first tried to check this with

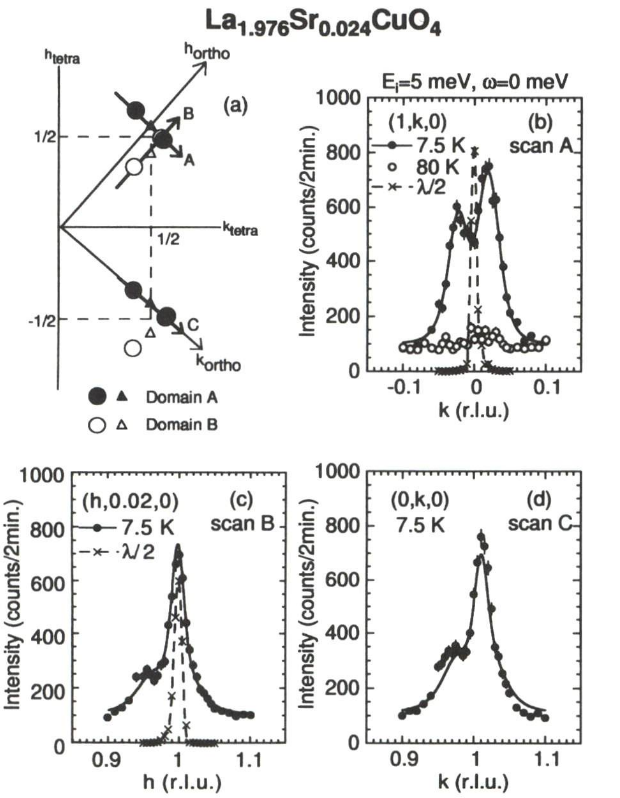

Fig. 4. (a) Diagram of the reciprocal lattice in the $(HK0)$ scattering zone. Filled and open symbols are for domains A and B, respectively. The triangles and circles correspond to nuclear and magnetic Bragg peaks, respectively. The thick arrows show scan trajectories. Transverse (b) and longitudinal elastic scans (c) and (d) around (1,0,0) and (0,1,0) at 7.5 K (filled circles) and 80 K (open circles) in $La_{1.976}Sr_{0.024}CuO_4$. The crosses represent the higher-order Bragg peaks observed at (1,0,0) by removing the Be filters. The broken lines are guides to the eyes. The peak width represents the instrumental resolution. The solid lines are the results of fits to a convolution of the resolution function with 3D squared Lorentzians with ξ'_a=94.9 Å, ξ'_b=39.9 Å, ξ'_c=3.15 Å, and ϵ=0.0232 r.l.u. [17].

$La_{1.98}Sr_{0.02}CuO_4$ sample[16], which was grown by flux method in a platinum crucible. Due to a small magnetic impurity phase with a long-range AF ordering, it was difficult to perform measurements in the $(HK0)$ scattering plane, which is necessary to determine whether the magnetic correlations are IC or not. Matsuda *et al.* have then performed neutron scattering experiments in $La_{1.976}Sr_{0.024}CuO_4$[17], which was grown by traveling solvent floating zone technique. The crystal has a twin structure and there exist two domains. The two domains are estimated to be equally distributed. Figure 4(a) shows the scattering geometry in the $(HK0)$ scattering plane. The filled triangles correspond to the (1,0,0) and (0,1,0) Bragg points from domain A while the open triangles denote the (1,0,0) and (0,1,0) Bragg points from domain B. Below ~40 K elastic magnetic peaks develop and at low temperatures the peaks are clearly resolved at the IC positions $(1,\pm\epsilon,0)$ and $(0,1\pm\epsilon,0)$ with ϵ ~0.0232. This corresponds to the same diagonal one-dimensional spin modulation observed in $La_{1.95}Sr_{0.05}CuO_4$ which has ϵ ~0.064.[15] The open and filled circles in Fig. 4(a) correspond to the IC magnetic peaks from the two domains in the $(HK0)$ zone. Figures 4(b)-(d) show transverse and longitudinal elastic scans around (1,0,0) and (0,1,0). Two peaks are observed in the transverse scan A while one intense peak together with a weak shoulder on the low-h side is observed in the longitudinal scans B and C. The instrumental resolution at (1,0,0) can be estimated from higher-order reflections, which in turn are measured by removing the Be filters. As illustrated in Figs. 4(b) and 4(c), the magnetic peaks are much broader than the resolution along both h and k.

The solid lines in Figs. 4(b)-(d) are the results of fits to a convolution of the resolution function with 3D squared Lorentzians. The two intense peaks in Fig. 4(b) originate primarily from the magnetic signals at $(1,1\pm\epsilon,0)$ in domain A while the weak shoulder in Fig. 4(c) originates from magnetic signals at $(0,1-\epsilon,\pm1)$ in domain B. The relatively intense peaks observed at $(0,1\pm\epsilon,0)$ occur because of the short correlation length along the c axis, which in turn makes the $(0,1\pm\epsilon,L)$ with L odd magnetic peaks broad along the c axis. The instrumental resolution function is also elongated along the c axis so that the magnetic signals are effectively integrated. The observed data are fitted with ξ'_a=94.9±4.0 Å, ξ'_b=39.9±1.3 Å, ξ'_c=3.15±0.08 Å, and ϵ=0.0232±0.0004 r.l.u., where ξ'_a, ξ'_b, and ξ'_c represent the inverse elastic peak widths in Q along the a, b, and c axes, respectively. The calculation reproduces the observed profiles quite well. ¿From these results, it is confirmed that the diagonal spin modulation occurs universally across the spin-glass phase.

The incommensurability ϵ corresponds to the inverse modulation period of the spin density wave. Here, ϵ is defined in orthorhombic notation so that $\epsilon = \sqrt{2} \times \delta$ where δ is defined in tetragonal units. As shown in Fig. 1, δ follows reasonably well the linear relation $\delta = x$ over the range $0.03 \leq x \leq 0.12$ which spans the insulator-superconductor transition. In a charge stripe model this corresponds to a constant charge per unit length in both the diagonal and collinear stripe phases, or equivalently, 0.7 and 0.5 holes per Cu respectively because of the $\sqrt{2}$ difference in Cu spacings in the diagonal and collinear geometries. Our value for x=0.024 falls slightly below the $\delta = x$ line and indeed it corresponds to ~1 hole/Cu as in $La_{2-x}Sr_xNiO_4$ where there is ~1 hole/Ni.[18] We note that Machida and Ichioka predict 1 hole/Cu throughout the diagonal stripe phase.[19]

2.2 *Spin structure*

The magnetic correlations perpendicular to the CuO_2 plane are now considered. Matsuda *et al.* performed a detailed study on the magnetic structure in the spin-glass $La_{1.98}Sr_{0.02}CuO_4$.[16] Figures 5(a) and 5(b) show the L dependence of the magnetic elastic peaks in $La_{1.98}Sr_{0.02}CuO_4$ measured at $(1,0,L)$ and $(0,1,L)$ at 1.6 K, respectively. The background estimated from the high temperature data (60 K) was subtracted so that the remaining signal is purely magnetic. These scans probe the between-plane magnetic correlations. Broad peaks are observed at (1,0,*even*) where magnetic Bragg peaks exist in La_2CuO_4. There are some characteristic features. Firstly the peaks are broad, indicating that the spin cor-

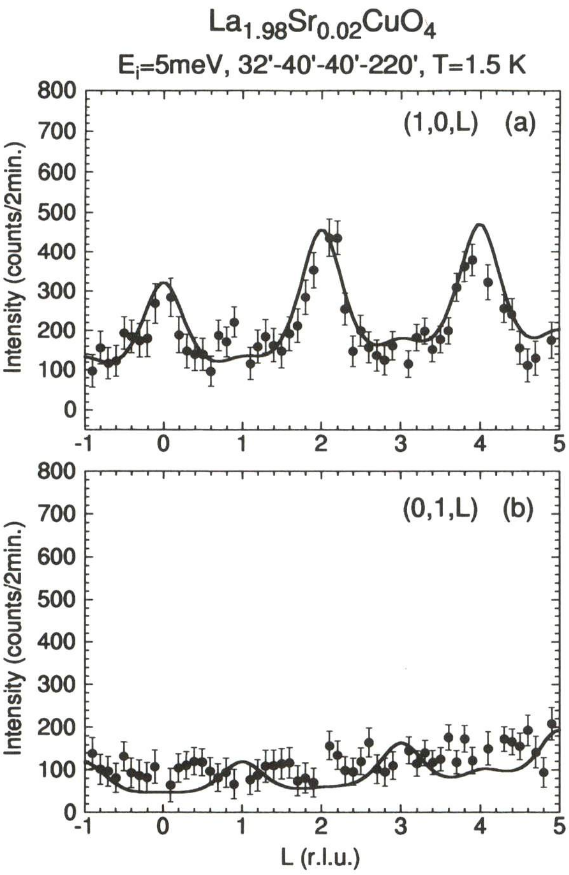

Fig. 5. Elastic scans along $(1,0,L)$ (a) and along $(0,1,L)$ (b) at 1.6 K in $La_{1.98}Sr_{0.02}CuO_4$. The background intensities measured at 60 K are subtracted. The solid lines shows the results of fits to a convolution of the resolution function with 3D squared Lorentzians with ξ'_a=160 Å, ξ'_b=25 Å, and ξ'_c=4.7 Å [16].

relations along the c axis are short-ranged. Secondly, the magnetic intensity at (1,0,*even*) initially increases with increasing L, in contrast to the behavior found for the magnetic Bragg intensities in pure La_2CuO_4. Lastly, the magnetic intensities at $(1,0,L)$ are much larger than those at $(0,1,L)$. From these results, one can deduce that spin clusters are formed in $La_{1.98}Sr_{0.02}CuO_4$. However, the spin clusters have a different geometrical structure from that in pure La_2CuO_4.

The magnetic Bragg intensity is proportional to

$$\left[\mathrm{S}_\perp f(Q) \sum_j \exp(i\mathrm{Q}\cdot\mathrm{R}_j) \right]^2 \tag{2.1}$$

where $\mathrm{S}_\perp$, $f(Q)$, and R_j are the copper spin component perpendicular to Q, the magnetic form factor, and the copper ion positions, respectively. In pure La_2CuO_4, the magnetic intensities at $(1,0,even)$ are just proportional to $f(Q)^2$, which is approximately constant for the range of L's considered here[20], since the copper spins point along the b axis perpendicular to the $(H0L)$ scattering plane and $\sum \exp(iQ\cdot\mathrm{R}_j)$ at $(1,0,even)$ is calculated to be constant from the 3D spin structure with the antiferromagnetic propagation vector $\tau \parallel a_{\mathrm{ortho}}$.

Table I. Hole concentration dependence of the static spin correlation length in $La_{2-x}Sr_xCuO_4$. – means that the peak width is too broad to determine ξ'_c. It is noted that ξ'_b in the x=0.02 sample is obtained on the assumption that the magnetic signal is commensurate. This value could become larger if the magnetic correlations are incommensurate.

x	ξ'_a (Å)	ξ'_b (Å)	ξ'_c (Å)
0.02[a]	160	25	4.7
0.024[b]	94.9±4.0	39.9±1.3	3.15±0.08
0.05[c]	33	25	–

[a]Ref. 16
[b]Ref. 17
[c]Ref. 15

The simplest model to explain the increase of the intensity with increasing L along both $(1,0,L)$ and $(0,1,L)$ is that the cluster antiferromagnetic spin is randomly directed within the ab plane. In this case, the intensity would vary like

$$[\mathrm{S}_\perp f(Q)]^2 = \frac{1}{2}\left[1+\sin^2\theta(L)\right] S^2 f(Q)^2 \tag{2.2}$$

where $\theta(L)$ is the angle that the Q-vector of the $(1,0,L)$ or $(0,1,L)$ reflection makes with the ab plane. We will justify this model after first discussing the spatial geometry of the frozen clusters. We should note that a result equivalent to Eq. (2.2) is obtained by fixing the spin direction along $(H,H,0)$ or by assuming equal admixtures of 3D correlated phases where the spin vector S is along or perpendicular to $\tau (\parallel a_{\mathrm{ortho}})$. The solid lines in Figs. 5(a) and 5(b) are the calculated profiles using as the intrinsic line shape 3D squared Lorentzians convoluted with the instrumental resolution function. The parameters used are ξ'_a=160 Å, ξ'_b=25 Å, and ξ'_c=4.7 Å. In the Néel state of pure La_2CuO_4 the spin is along b_{ortho} while just above T_N=325 K, that is, at 328 K when the correlation length is about 800 Å (Ref.[21]) the spin is randomly oriented in the ab plane. Because of the latter result it seems physically plausible that in the frozen spin clusters below 40 K in $La_{1.98}Sr_{0.02}CuO_4$ the spin direction would also be random. This is consistent with the fact that the net Ising anisotropy favoring the b_{ortho} axis from the Dzyaloshinsky-Moriya interaction is only about 0.1 K in energy. We should note that in all cases we assume that the propagation vector of the AF order is along a_{ortho} in order to account for the pronounced peaks at $(1,0,L)$ for L even alone.

The static spin correlation lengths, which are inverse peak widths in q, in $La_{2-x}Sr_xCuO_4$ (x=0.02, 0.024, and 0.05) are summarized in Table 1. With increasing hole concentration, the peak width both parallel and perpendicular to the CuO_2 plane becomes rapidly broadened. In $La_{1.95}Sr_{0.05}CuO_4$, the L-scan shows that the peak width along L is much broader than that in $La_{1.98}Sr_{0.02}CuO_4$, indicating that the magnetic correlations are two-dimensional.[15]

There are at least two possible origins of the finite correlation lengths in the CuO_2 plane for the static order in the spin-glass $La_{2-x}Sr_xCuO_4$. The first is that the

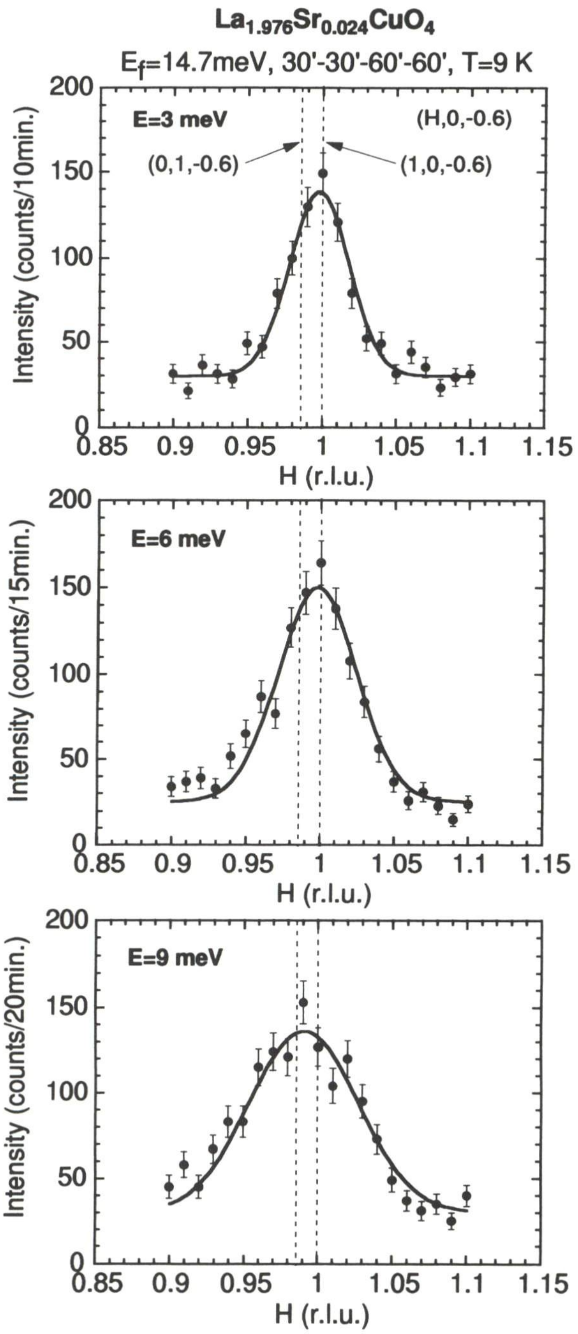

Fig. 6. Inelastic scans along $(H, 0, -0.6)$ at 9 K as a function of energy in $La_{1.976}Sr_{0.024}CuO_4$. The solid lines are guides to the eye. The broken lines show the centers of the peaks (1,0,−0.6) and (0,1,−0.6) determined from the nuclear Bragg peak positions.

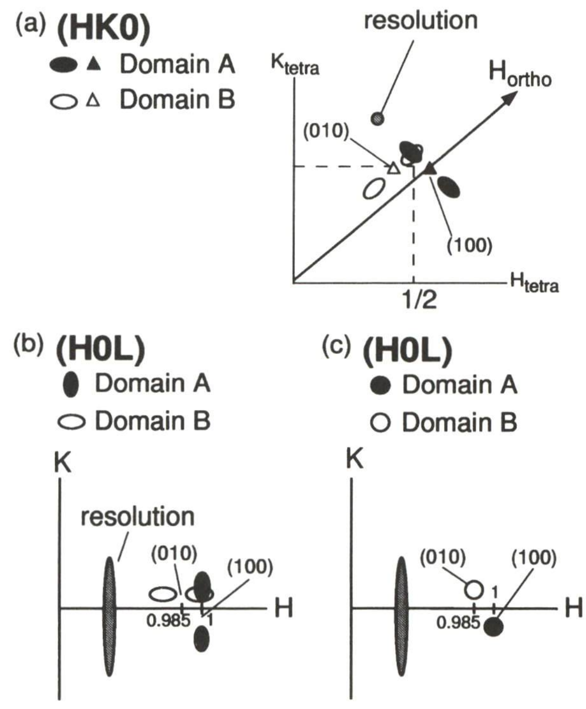

Fig. 7. The schematic configuration of the magnetic peaks in the $(HK0)$ and $(H0L)$ scattering zones. The instrumental resolution is elongated perpendicular to the scattering plane. The ellipsoids and circles represent magnetic peaks. (a) and (b) show scattering configurations in the IC phase. As shown in the text, the IC magnetic peaks are anisotropic. In the commensurate phase (c), the peaks are considered to be isotropic.

lengths simply measure the spin decoherence distance of the AF spin clusters. The second is that the disorder originates primarily from a random distribution of stripe spacings and orientations as discussed by Tranquada *et al.*[22] Further experiments and theoretical calculations will be required to choose between these possibilities.

§3. Magnetic excitations

We now consider how the inelastic magnetic correlations are in the spin-glass phase of $La_{2-x}Sr_xCuO_4$. Constant-ω scans were performed in $La_{1.976}Sr_{0.024}CuO_4$.[23] Figure 6 shows neutron inelastic scans at the energies 3, 6, and 9 meV measured at 9 K.A sharp excitation peak is centered at H=1 at ω=3 and 6 meV. On the other hand, the peak position is shifted to lower H(∼0.99) at ω=9 meV. It is possible that this behavior is explained as follows. At 3 and 6 meV, the magnetic peaks exist at IC positions as observed in the elastic scans in the $(HK0)$ zone as shown in Fig. 7(a). Then the instrumental resolution elongated vertically integrates the magnetic signal around H=1 very effectively in the $(H0L)$ zone, as shown in Fig. 7(b), so that the sharp and intense peak is centered at H=1. On the other hand, the magnetic correlations are considered to be commensurate and isotropic at 9 meV as shown in Fig. 7(c). In this case, there exist two equi-intense peaks at H=0.985 and 1 so that one broad peak is located at H ∼0.99. ¿From this result, it is considered that there occurs an incommensurate-commensurate transition between 6 and 9 meV. Further measurements are needed to clarify the incommensurate-commensurate transition in more detail.

§4. Summary

We find that a short range static one-dimensional diagonal spin modulation exists at low temperature across the entire insulating spin-glass region in $La_{2-x}Sr_xCuO_4$. Further, the charge density per unit length is approximately constant except at the lowest Sr concentration of

x=0.024 where the charge density increases to about 1 hole/Cu. This diagonal spin modulation state thus is a generic feature which must be understood as a precursor to high temperature superconductivity.

Acknowledgments

This work has been performed in collaboration with R. J. Birgeneau, P. Böni, Y. Endoh, M. Fujita, M. A. Kastner, Y. S. Lee, S.-H. Lee, G. Shirane, S. Wakimoto, and K. Yamada. This study was supported in part by the U.S.-Japan Cooperative Program on Neutron Scattering operated by the United States Department of Energy and the Japanese Ministry of Education, Science, Sports and Culture and by a Grant-in-Aid for Scientific Research from the Japanese Ministry of Education, Science, Sports and Culture.

1) M. A. Kastner, R. J. Birgeneau, G. Shirane and Y. Endoh: Rev. Mod. Phys. **70** (1998) 897.
2) D. Vaknin, S. K. Shinha, D. E. Moncton, D. C. Johnston, J. Newsam, C. R. Safinya and H. King: Phys. Rev. Lett. **58** (1987) 2802.
3) R. J. Birgeneau, M. Greven, M. A. Kastner, Y. S. Lee, B. O. Wells, Y. Endoh, K. Yamada and G. Shirane: Phys. Rev. B **59** (1999) 13788.
4) A. Aharony, R. J. Birgeneau, A. Coniglio, M. A. Kastner and H. E. Stanley: Phys. Rev. Lett. **60** (1988) 1330.
5) B. J. Sternlieb, G. M. Luke, Y. J. Uemura, T. M. Riseman, J. H. Brewer, P. M. Gehring, K. Yamada, Y. Hidaka, T. Murakami, T. R. Thurston and R. J. Birgeneau: Phys. Rev. B **41** (1990) 8866.
6) B. Keimer, N. Belk, R. J. Birgeneau, A. Cassanho, C. Y. Chen, M. Greven, M. A. Kastner, A. Aharony, Y. Endoh, R. W. Erwin and G. Shirane: Phys. Rev. B **46** (1992) 14034.
7) K. Yamada, C. H. Lee, K. Kurahashi, J. Wada, S. Wakimoto, S. Ueki, H. Kimura, Y. Endoh, S. Hosoya, G. Shirane, R. J. Birgeneau, M. Greven, M. A. Kastner and Y. J. Kim: Phys. Rev. B **57** (1998) 6165.
8) S.-W. Cheong, G. Aeppli, T. E. Mason, H. A. Mook, S. M. Hayden, P. C. Canfield, Z. Fisk, K. N. Klausen and J. L. Martinez: Phys. Rev. Lett. **67** (1991) 1791.
9) H. Yoshizawa, S. Mitsuda, H. Kitazawa and K. Katsumata: J. Phys. Soc. Jpn. **57** (1988) 3686.
10) R. J. Birgeneau, Y. Endoh, Y. Hidaka, K. Kakurai, M. A. Kastner, T. Murakami, G. Shirane, T. R. Thurston and K. Yamada: Phys. Rev. B **39** (1989) 2868.
11) T. Suzuki, T. Goto, K. Chiba, T. Shinoda, T. Fukase, H. Kimura, K. Yamada, M. Ohashi and Y. Yamaguchi: Phys. Rev. B **57** (1998) 3229.
12) H. Kimura, K. Hirota, H. Matsushita, K. Yamada, Y. Endoh, S.-H. Lee, C. F. Majkrzak, R. Erwin, G. Shirane, M. Greven, Y. S. Lee, M. A. Kastner and R. J. Birgeneau: Phys. Rev. B **59** (1999) 6517.
13) J. M. Tranquada, J. D. Axe, N. Ichikawa, Y. Nakamura, S. Uchida and B. Nachumi: Phys. Rev. B **54** (1996) 7489.
14) S. Wakimoto, R. J. Birgeneau, Y. Endoh, P. M. Gehring, K. Hirota, M. A. Kastner, S. H. Lee, Y. S. Lee, G. Shirane, S. Ueki and K. Yamada: Phys. Rev. B **60** (1999) R769.
15) S. Wakimoto, R. J. Birgeneau, M. A. Kastner, Y. S. Lee, R. Erwin, P. M. Gehring, S. H. Lee, M. Fujita, K. Yamada, Y. Endoh, K. Hirota and G. Shirane: Phys. Rev. B **61** (2000) 3699.
16) M. Matsuda, Y. S. Lee, M. Greven, M. A. Kastner, R. J. Birgeneau, K. Yamada, Y. Endoh, P. Böni, S.-H. Lee, S. Wakimoto and G. Shirane: Phys. Rev. B **61** (2000) 4326.
17) M. Matsuda, R. J. Birgeneau, Y. Endoh, M. Fujita, M. A. Kastner, G. Shirane, S. Wakimoto and K. Yamada: unpublished.
18) J. M. Tranquada, D. J. Buttrey and V. Sachan: Phys. Rev. B **54** (1996) 12318.
19) K. Machida and M. Ichioka: J. Phys. Soc. Jpn. **68** (1999) 2168.
20) T. Freltoft, G. Shirane, S. Mitsuda, J. P. Remeika and A. S. Cooper: Phys. Rev. B **37** (1988) 137.
21) See for example, the analogous data in pure La_2CuO_4 above T_N in Fig. 2 of Ref. 3.
22) J. M. Tranquada, N. Ichikawa and S. Uchida: Phys. Rev. B **59** (1999) 14712.
23) M. Matsuda, R. J. Birgeneau, Y. Endoh, M. Fujita, M. A. Kastner, G. Shirane, S. Wakimoto and K. Yamada: unpublished.
24) S. Wakimoto and S.-H. Lee: (private communication).